June 2014 Status Report and Proposal For EIC Calorimeter Development

The EIC Calorimeter R&D Consortium

– Contact Persons: H.Z. Huang huang@physics.ucla.edu
C. Woody woody@bnl.gov

S.Boose, E. Kistenev, J.Haggerty, C.Pinkenberg, S. Stoll, and C. Woody
(PHENIX Group, Physics Department)
E. Aschenauer, S. Fazio and Alexander Kiselev
(Spin and EIC Group, Physics Department)
Y. Fisyak
(STAR Group, Physics Department)
Brookhaven National Laboratory

F. Yang and L. Zhang and R-Y. Zhu
California Institute of Technology

T. Horn
The Catholic University of America and
Thomas Jefferson National Accelerator Facility

W. Jacobs, G. Visser and S. Wissink
Indiana University

C. Munoz-Camacho
IPN Orsay, France

S. Heppelmann
Pennsylvania State University

C. Gagliardi and M.M. Mondal
Texas A&M University

L. Dunkelberger, H.Z. Huang, K. Landry, Y. Pan, S. Trentalange, O. Tsai
University of California at Los Angeles

Y. Zhang, H. Chen, C. Li and Z. Tang
University of Science and Technology of China

H. Mkrtychyan
Yerevan Physics Institute

Overview

The EIC Calorimeter Consortium has three major research directions: 1) R&D effort to build compact sampling EM Calorimeter; 2) the development of crystal calorimeter for the measurement scattered electrons; and 3) Monte Carlo simulations for physics capabilities, detector design options and performance requirements. Here we present our progress report and proposal for the coming year.

Two teams have been working on the compact EMCal design and prototyping. The RD1 team (UCLA/IU/TAMU/PSU/BNL) has been working on a W-powder/Scintillating fiber based SPACal-type calorimeter geometry and the BNL PHENIX Team has been working on a Tungsten plate geometry calorimeter. A beam test run was carried out at FNAL in Feb-Mar 2014. We report the test beam results from the prototyping of these EMCal designs. Given the constraints on the manpower and resources and the test beam results, we agreed to consolidate our EMCal design effort and will focus on the SPACal design with W-powder/Scintillating fibers in our future plans.

For the crystal detector development significant progress has been made with the BSO crystals by the USTC group. Initial production of BSO crystals from SICCAS had been characterized. We continue with Monte Carlo simulations to understand the performance of the crystals. A major concern is the yield of high quality BSO crystals from SICCAS and their radiation hardness in the EIC environment.

A new team with considerable experience in crystal detectors joined the EIC calorimeter consortium to take upon the task of investigating PWO crystals from both SICCAS and Crytur, which uses different methods to grow these crystals. It is known that the quality of the crystals including PWO crystal's optical properties and the radiation hardness seems to depend critically on the method of growth. The evaluation of PWO crystals from these vendors within the context of EIC physics and environment will be an important task for the consortium. A new proposal and budget request from this team is included in this document. The calorimeter consortium strongly endorses these proposed R&D activities.

The Monte Carlo simulation project by the BNL team aims at the development of tracking and calorimeter requirements for an EIC detector. A separate report covering both the tracking and calorimeter related simulations will be submitted by the BNL group. In addition, a new effort on simulation of the radiation levels for an EIC detector will be initiated by this team.

We note that we have regular meetings among the tracking and calorimeter consortia. Our future efforts will focus on 1) study the SiPM performance and radiation effects on the SiPM read-out scheme; 2) improvement to the front-end electronics design for the SiPM read-out system; 3) improvements to the energy resolution of a sampling EMCal and prototyping for another beam test; 4) characterizing properties of BSO and PWO crystals; and 5) Monte Carlo simulations of physics capabilities and the radiation environment from both physics collisions and beam-related radiations. We hope to continue the synergy among the research groups in the calorimeter consortium. We also recognize that we need additional research groups if we are to build an actual EIC calorimeter system. We will reach out to more groups and hope to expand our R&D activities in the coming year.

Compact EMCal R&D Project

RD1 Team Progress Report
Reporting Period: From 12/13/2013 to 06/27/2014

Project Name: Development of a New Technology for Fiber Sampling Calorimeters for EIC

Project Leader: Huan Z. Huang

Date: 06/27/2013

1. Overview.

Over the past six months the main goal of our RD1 collaboration was to carry out a test run at FNAL and analyze the test run data. Two new EM calorimeter matrices (16 towers for the forward calorimeter) and 18 wedge-type towers for a barrel EM calorimeter prototype were constructed during the summer/fall of 2013 at UCLA. The parallel R&D for the STAR forward upgrade led to construction of a compensated hadronic calorimeter prototype consisting of 16 towers (4 interaction lengths deep, each tower 10 x 10 cm^2). This same technology is now adopted for hadronic calorimeters in the outgoing hadron forward region of a dedicated EIC detector system. All three calorimeter prototypes were equipped with compact readout systems utilizing silicon photomultipliers. For the EM section, each tower was read out with four Hamamatsu 3 mm x 3 mm sensors. Each HAD tower was readout with eight such sensors.

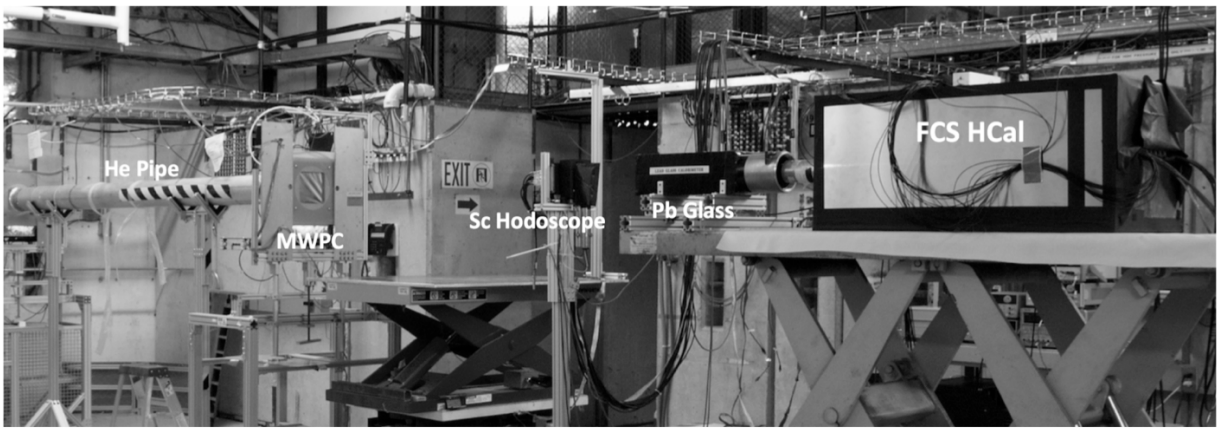

Figure 1.1 Participants of the test run at FNAL, and experimental setup at the beam line on March 1, 2014.

The analysis of the test run data is in progress (bulk of the data were analyzed by graduate students and postdocs and now continued by undergraduate student). The comparison of the test run data and MC

predictions was started (curried out by BNL EIC group and UCLA postdoc). For that, the exact test run geometry was put independently in GEANT4 and EIC MC software packages.

2. *Detector prototypes and test beam results*

A detailed description of construction technique for EM prototypes was given in our previous reports. Figure 1.2 shows two EM prototypes tested at FNAL.

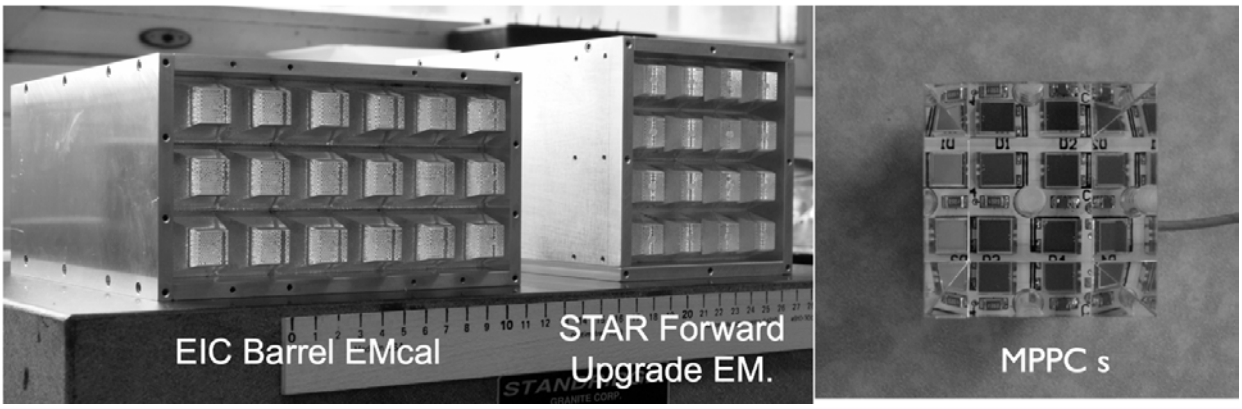

Figure 1.2 Eighteen channels, 18 X_0 deep EM prototype of the central barrel calorimeter for a dedicated EIC detector (left). A sixteen channels, 23 X_0 deep prototype of the forward EM calorimeter for FCS (right). Both prototypes used similar light collection schemes and frontend electronics. Compact readout for EM section shown on the right. EM FEE board with four MPPCs attached to a light guide. View from the base of the light guide.

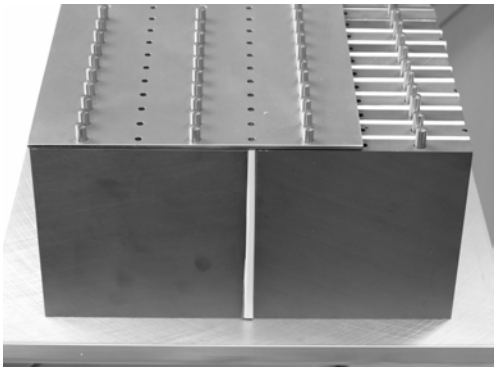

Figure 1.3 Basic mechanical structure of HCAL

Since the dedicated EIC detector adopted our HCAL technique, we are giving a more detailed description of the prototype (compare to our previous report) here. The HCal section is a stack of layers of absorber and scintillation plates. The easiest way to describe the assembly process is to imagine building an entire HCal block from LEGO style parts layer by layer. Figure 1.3 shows the basic mechanical structure of the HCal mechanical prototype.

Holes in the bottom base plate of the detector provide locations of the absorber plates. Each absorber plate has four holes for dowel pins, two at the bottom and two at the top. Steel dowel pins (5 mm in diameter) position the absorber plates with respect to the bottom base and top steel master plates.

Figure 1.4 HCAL assembled in place in 8 hours.

A single master plate covers one and a half rows of HAD towers, providing interlinks: between all absorber plates within one tower, between front and back steel plates of the HAD section and between adjacent rows of the HAD towers. The thickness of the absorber plates is 10 mm. They made of lead antimony alloy (4% Sb) and painted with a white diffusive reflective paint (Sherwin Williams F63WC134). The gap between two adjacent absorber plates is 3.1 mm. A 2.5 mm thick scintillation plates (EJ-212) was placed inside these gaps. There are 63 absorber pates and 64 scintillation plates in a single

HCal tower. Scintillation light from a single tower is collected with a 3 mm thick wavelength shifting (WLS) plate (EJ-280), which is placed in the gap between the two adjacent HCal towers as shown in figure 1.3. All scintillation and WLS plates are “floating” within each layer (there are no mechanical loads on these elements). Figure 1.4 shows an assembled HCal prototype. We assembled this prototype in place (FNAL test beam) to validate the construction technique. It took about eight hours for four people to build the sixteen channels HCal prototype from bare parts at the test beam site.

We tested the response of the FCS system to hadrons, electrons and muons in the energy range 3-32 GeV. Electrons were identified with a differential Cherenkov counter (standard equipment at the MTBF). The impact position was defined by a scintillator XY hodoscope (4.9 mm wide scintillatior square rods readout by SENSL SiPMTs). We minimized the amount of materials upstream of the calorimeters in the beam line to about 4 cm of scintillation counters. Additionally, FTBF personnel installed a He filled beam pipe between our apparatus and the upstream Cherenkov counter. The initial setup of our apparatus on the beam line is shown in figure 1.1. Two MTBF MWPC (one is seen in figure 1.1) were used as additional monitoring devices during the beam energy scans to track reproducibility of the beam settings at different energies. The HCal was oriented with a fixed angle (2.5 degrees) between the beam and primary axis of the HCal towers. The EMcal prototype was attached to the front steel plate of the HCal. The angle between the axis of EM tower and beam was kept at 4 degrees. All channels of the FCS were equipped with a LED monitoring system. LED monitoring signals and pedestals events were continuously recorded with a rate about 1 Hz most of the time during the test run. Preliminary analysis of these data shows that stability of the gain for HCal and EMcal front end electronics was better than 1% during a typical twelve hours shift of data taking as shown on Fig 1.5.

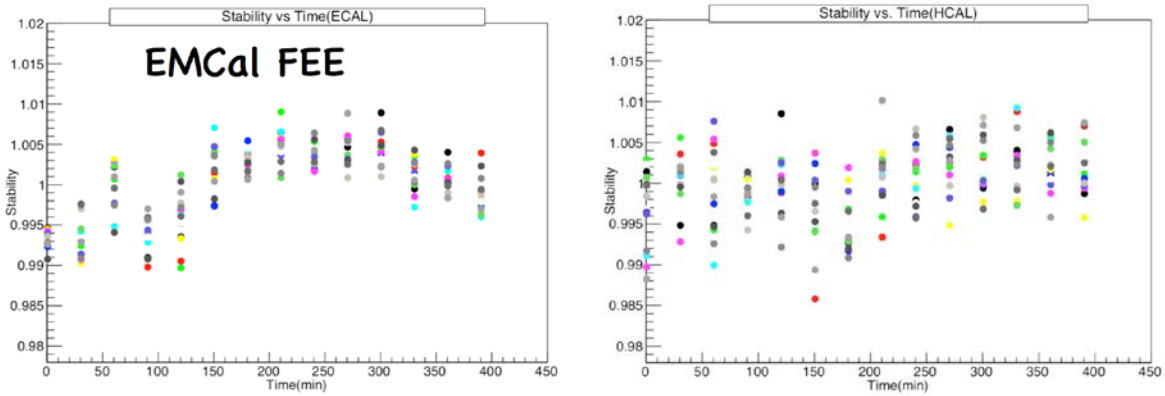

Figure 1.5 Stability of the gain for HCAL and EMcal during data taking.

All MPPC’s were tested with a laser system prior to the test run. With this system we measured that the gain of the MPPC assemblies for both HCal and EM prototypes were set equal to within 1%. We found that no additional tower-by-tower calibration of the EM prototypes with the beam was required. This was expected after our previous beam test in 2012 when we measured excellent internal homogeneity of the EM modules built with our technique. The HCal required additional tower-by-tower equalizations with MIPs. For that an absorber was inserted into the beam line (8 GeV muon mode for the MT6 test line). A MIP peak was selected in each HCal tower using an isolation requirement (a single muon hit in a tower with no other energy deposition in the entire HCal). For calibrations with MIPs the EM prototype was removed from the beam line. We found that quite large corrections at the level of approximately 20% were required on top of calibrations made prior to the test run. About 10% of this shift can be explained by the alignment of the WLS plate and the MPPCs (both have a 3 mm active area, about 250 microns misalignment is possible

due to positioning of the MPPCs on the FEE board). The rest could be attributed to the quality of optical components. One possible source is a difference in the response of the WLS tiles used in different HCal towers (concentration of dopants and attenuation length has not been measured for every WLS tile used in the HCal, we assumed that they are all identical).

As we described in our previous report we developed a new compact readout for the FCS. For both EM and HCal sections we decided to use silicon photomultipliers (Hamamatsu Multi Pixel Photon Counters (MPPC) S10931-025p). They are very compact, fast and insensitive to the magnetic field and sufficiently radiation hard. The measured light yield (with a very efficient light collection scheme and PMTs) from the EM prototype in the test run in 2012 was 2000 p.e./GeV. We estimated that with 4 MPPC per tower for EM section and with 8 MPPC per tower for the HCal section we will collect enough light to keep the contribution form the photo-statistics to the energy resolution of the detector at a negligibly small level. The geometrical efficiency (ratio of active area of eight MPPCs to the output surface area of the WLS plate) of the light collection scheme for HCal is 8.2% and ~21% for EMcal towers.

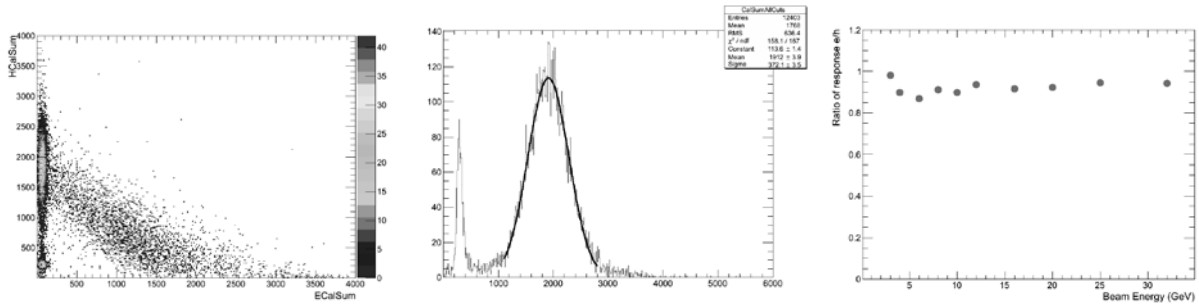

Figure 1.6 Response of FCS prototype to hadrons. Energy deposition in Hcal section (Y-axis) vs energy deposition in EMcal section (X-axis) for 12 GeV hadrons (left panel). A weighted sum of energy deposited in EM and HCal section for 12 GeV hadrons (center panel). Ratio of response of FCS to electrons vs hadrons (**e/h** ratio) vs beam energy (right panel).

The response of the FCS to hadrons is illustrated in figure 1.6. In an ideal completely compensated calorimeter system the reconstructed energy of the incoming hadron is a simple sum of the energy deposited in the EM and HCal sections (assuming that the response in both sections is the same and energy independent). To obtain the best energy resolution for hadrons in the FCS we found that a weighting factor for the EM section should be energy dependent. It changes from about 2 to 1.2 for beam energy range 3 to 20 GeV and stays flat after that. With this energy dependent weighting of the energy deposited in the EM section we measured the e/h ratio for the FCS to be close to 0.95 and almost constant above 10 GeV as seen in figure 1.6 in the right panel. We have not yet performed any corrections due to leakage in the transverse and longitudinal directions in the FCS. Qualitatively this result is close to MC predictions. However, in our previous MC model, we did not include any structural elements between EM and HCal sections, or the limited size of the prototype tested at FNAL. The questions of optimal weighting and the e/h ratio in the FCS still needs to be clarified with a MC with the exact geometry of the detectors used in the test run (**this is part of our future R&D activities**).

The response of the FCS to electrons is illustrated in figure 1.7. A bench test measurement prior the test run showed that with the compact scheme of readout with MPPCs, the non-uniformity of the light collection might be as high as 20% (the difference between the hottest spots just under the MPPCs and at the corners of the towers). We decided to proceed with this scheme anyway to measure the absolute light yield and later redesign the light collection scheme for the EM section depending on results of the test run (**this is part of our future R&D activities**). This was reported in

our previous report and we anticipated that a second iteration of the compact readout for EM sections would be required after the test run. Due to non-uniform light collection with MPPCs, the response of the EM section is dependent on impact position. The local coordinates of the impact position were determined using calorimeter information only. We used a logarithmic weighting method with a cut off parameter set at 3.8. For the results we present in this report, we corrected the energy deposition in the EM section according to impact position and restrict the impact area to the circle with a diameter 1.4 cm at the centre of the EM tower.

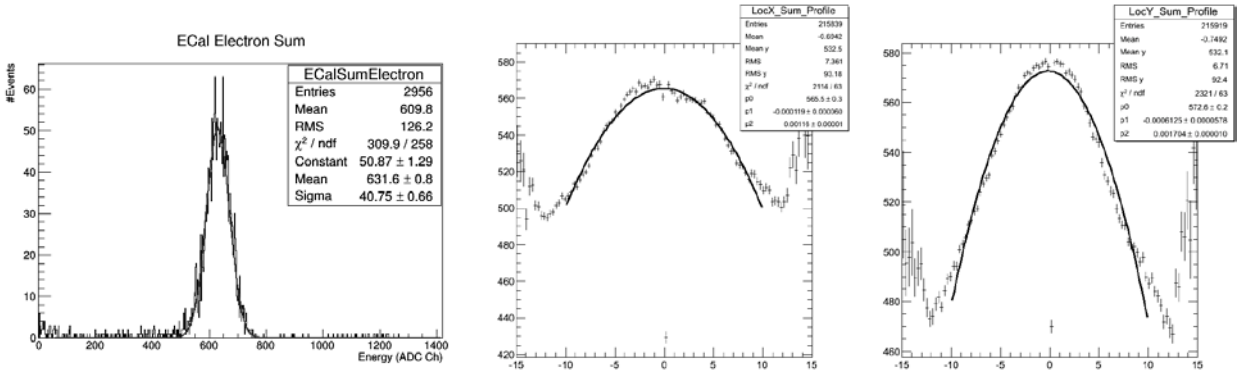

Figure 1.7 Response of FCS EM prototype to electrons. Energy deposition in the EM section for 4 GeV electrons, impact point restricted by the scintillation hodoscope to an area of 5 mm x 5 mm (left panel). Dependence of the energy deposited in the EM section vs impact position in local X coordinate (centre panel) and local Y coordinate (right panel).

The difference in the shapes of the response of the EM section in the X and Y directions is due to a tilt of the EM prototype of 4 degrees around the Y axis.

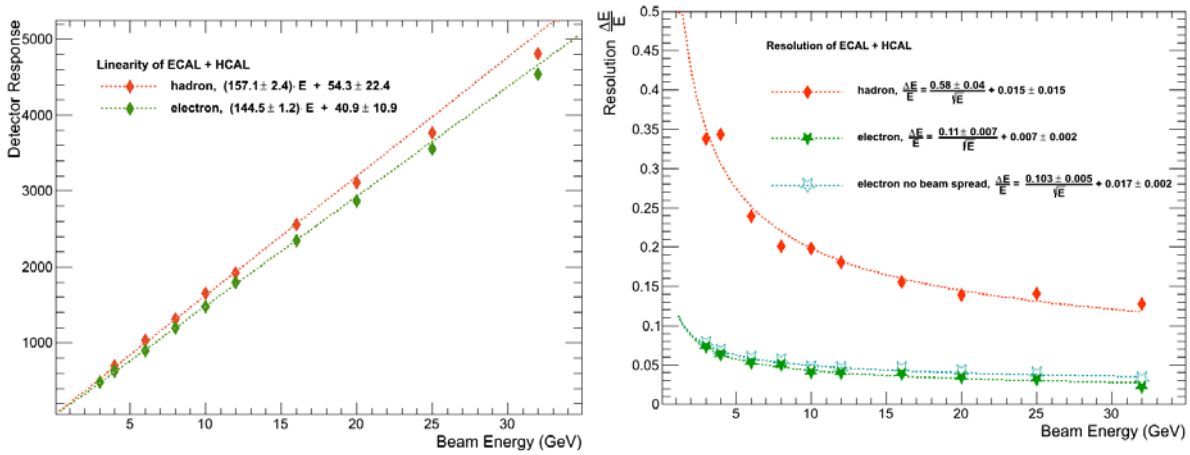

Figure 1.8 Response of the FCS prototype to electrons and hadrons vs energy (left panel). Energy resolution of the FCS for hadrons and electrons vs energy (right panel).

Summary plots illustrating the performance of the FCS prototype during the beam test are shown in figure 1.8. The response to electrons is almost linear, while the response to hadrons shows a clear deviation from linearity above 15 GeV. The most likely reasons for this deviation is the weighting procedure of the fraction of energy deposited in the EM section and leakage from the FCS. We tested the HCal section alone (with the EM section removed from the beam line) and did not observe a similar deviation form linearity in this energy range. The energy resolution of the

FCS to hadrons, shown in figure 1.8, is about 15% worse compared to MC predictions for the FCS at 10 GeV. One of the reasons is transverse leakage from the FCS prototype, which was not taken into account for the test beam results. We also should mention that the energy resolution of the FCS in MC depends on the physics list used in GEANT4. We used the LHEP physics list, which we believe provides the most accurate description of the FCS. However, this physics list will not be supported in future versions of GEANT due a number of problems. Instead, the FTFP physics list is recommended which we are investigating now. The proper modelling of the test beam data will require an accurate translation of the energy deposited in the scintillator to the number of detected photons (**tuning the MC is part of our future R&D activities**). The electromagnetic energy resolution of the FCS prototype is close to the MC predictions. There are two fits of our experimental results shown in figure 1.8. One assumed that the momentum spread of the beam is zero. In this case the stochastic term is close to 10% and the constant term is 1.7%. If we use our earlier (2012) estimates for the momentum spread of the beam of 2.7 % below 4 GeV and 2.3% above this value, then the stochastic term becomes 11% and constant term is close to zero.

The absolute light yield measured in the EM section is about 400 pixels/GeV with the front face of the EM prototype painted with the white diffusive paint BC-620. The measured absolute light yield for the HCal section is about 130 pixels/GeV. The light yield measured for the EM prototype is large enough that we can introduce a mask between the scintillation fibers and light guide to make the light collection more uniform (**this is part of our future R&D activities**). Given the fact that new generation of MPPCs already have much better PDE compared to MPPCs used in the test run (and anticipated future improvements in SiPMs), we believe that there is no need for any type of reflector at the end of the scintillation fibers. That significantly simplifies the construction of the EM section. According to our measurements in 2012, with EM prototypes equipped with a good mirror and with black tape at the end of the fibers, all degradation in the energy resolution can be explained by photo statistics, i.e. degradation of light attenuation length in the scintillation fibers is not critical in this case.

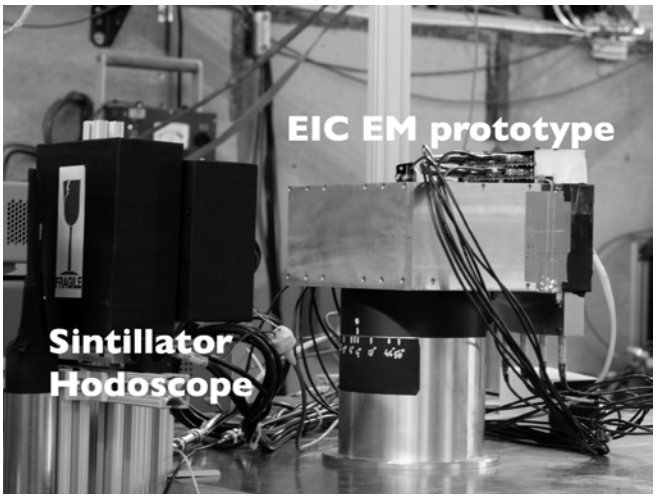

Figure 1.9 EIC EM prototype at the beam line.

Along with the FCS, we tested a prototype of the central barrel EM calorimeter for EIC. A picture of this prototype on the beam line is shown in figure 1.9. The goal of the test run was to measure the response of this detector at different impact angles. The design of the prototype shares the same technology with the EM prototype for the FCS, except the geometry of the towers. A wedge type geometry has always been technologically challenging for ScFi type calorimeters. We developed a simple construction technique for this type of geometry. The wedge shape is obtained by successively inclining meshes which form the matrix of scintillation fibers along the depth of the tower. This method is as simple as the method used for the traditional straight towers of the FCS. The sampling fraction and sampling frequency with inclined meshes slightly increases toward the front face of the towers. A MC shows that this variation of sampling structure has a minor effect on the energy resolution of the detector. The goal of the test run was to measure the energy resolution and absolute light yield in this detector as a function of impact angles. We performed beam energy scans for three different angles and tested three different light collection

schemes. Since the light collection scheme for this prototype is similar to FCS EM detector similar problems with non-uniformity of light collection were observed. At shallow impact angles (detector was rotated along Y vertical axis) the non-uniformities in response along X axis almost vanished. For the preliminary test beam results presented in this report, we limited the impact area in the Y direction to 5 mm to minimize effect of non-uniformity of light collection mentioned above and leakage from the prototype due to its limited size. Again, as in case of the forward EM prototype, calibration of individual towers with the beam was not required. This confirms that the method of coupling of the SiPM boards with the detector is very reliable. The same frontend board with SiPMs, which were used to readout forward EM prototype in the first portion of the test run, was then used in the second part of the test run to readout barrel EM prototype.

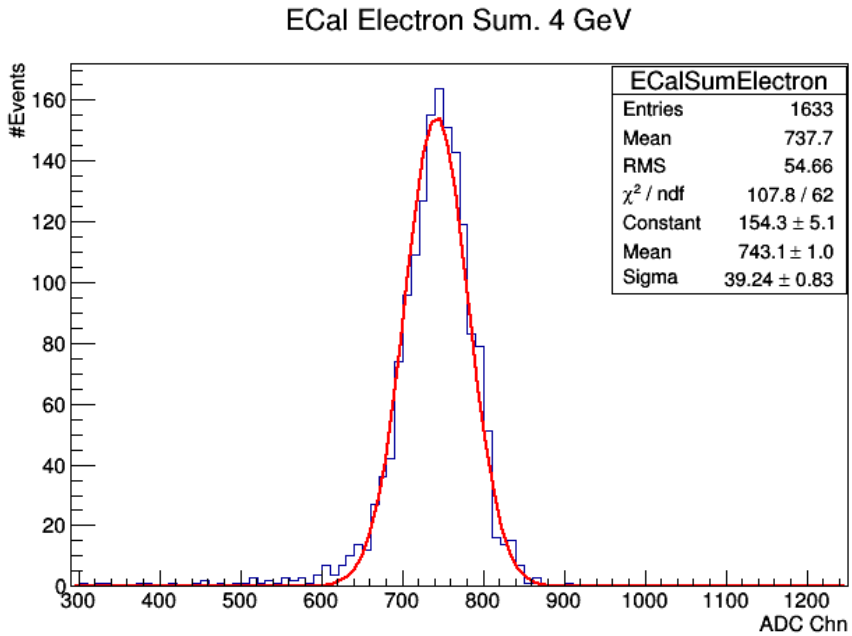

Figure 1.10 Typical amplitude spectrum in EIC EM prototype.

A typical amplitude spectrum for 4 GeV electrons is shown in figure 1.10. In the results shown below we did not perform clustering, i.e. the amplitude spectra is the sum of all eighteen channels. The cut off threshold on energy deposition in individual tower was set at about 13 MeV. The design of the central barrel EM calorimeter is non-projective in eta. Given the very small occupancy in the detector at EIC, this is not present a problem. A typical shower profiles at different impact angles are shown in figure 1.12

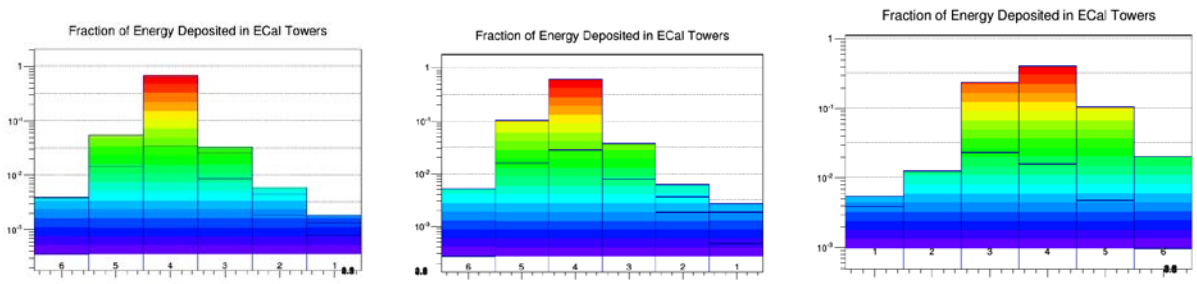

Figure 1.11 EM shower profiles at different impact angles.

At shallow impact angle, the multiplicity of hits (defined as energy deposition in individual tower above the noise), only slightly increases compare to close to 0 (projective geometry) impact angle as shown in figure 1.12.

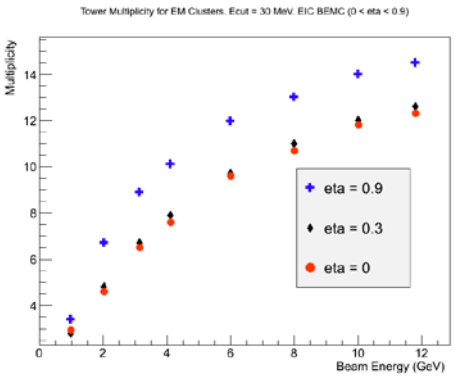

Figure 1.12 EM cluster multiplicity as a function of energy for different impact angles

Figure 1.13 summarizes the performance of the EM prototype for the central barrel EIC calorimeter during the test run. As predicted by the MC, the response of the detector only slightly depends on impact angle. A change in the slope for the fits at the left side of figure 1.12 can be explained by the slightly increased sampling fraction of the detector at more shallow impact angles. The energy resolution will be practically the same for the entire pseudo-rapidity range covered by the central barrel calorimeter for an EIC detector as shown at the right side in figure 1.13, which is again in reasonable agreement with MC predictions.

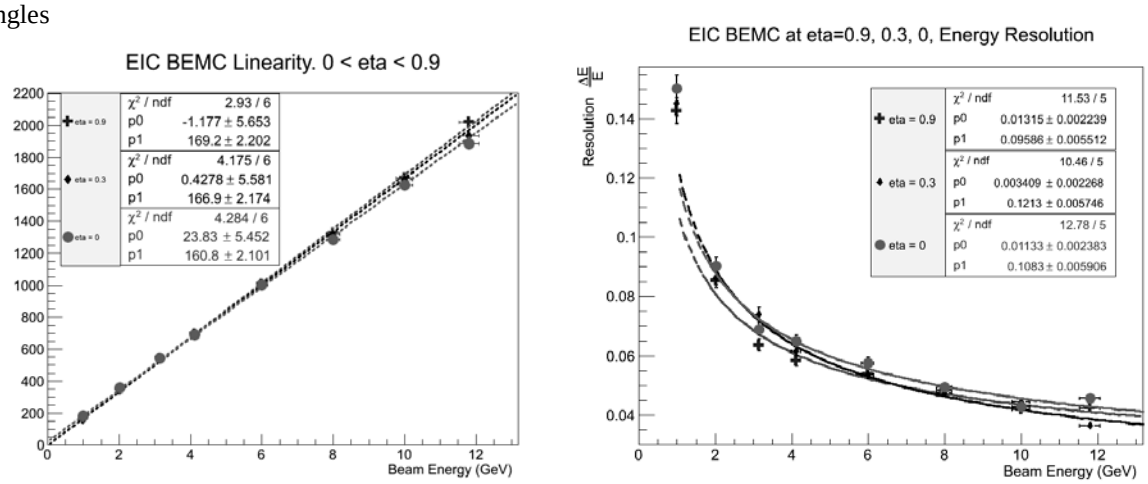

Figure 1.13 Response of the EM EIC prototype to electrons vs energy for different impact angles (left panel). Energy resolution (p0/√E + p1) of the EM EIC for electrons vs energy for different impact angles (right panel).

The light yield measured for this prototype was 430, 530 and 600 pixels/GeV depending on the type of reflector at the front face of the detector and materials surrounding light guides. The highest light yield was achieved with white diffusive paint at the front face of the detector (BC-620) and diffusive reflectors surrounding light guides. We found that multi clad scintillation fibers (Kuraray SCSF 78M) used for the EIC EM prototype only slightly improves the light yield compare to single clad fibers (Kuraray SCSF 78) used for the FCS EM prototype. There is no difference in performance of the EM prototypes when the readout was placed upstream (for FCS) or downstream (for EIC) of the detectors. It was important to compare the response of the detectors with different placement of the readout. With the readout placed upstream of the detector, all aspects of the mechanical design, integration and operation of the central barrel EM calorimeter becomes much simpler.

3. Summary from the test run

In 2012 we demonstrated a 'proof-of-principle' for a new simple and cost effective method of building compact scintillation fiber calorimeters utilizing tungsten powder. We continued

development of this technique and tested two new EM prototypes designed for the STAR forward upgrade and future central barrel EM calorimeter for a dedicated EIC detector. Both prototypes were successfully tested in the test run at FNAL in March of 2014. We also developed a new construction technique for a high-resolution lead scintillation tile hadronic calorimeter. The FCS system designed specifically for the STAR forward upgrade is now adopted for the forward calorimeter envisioned for the EIC dedicated detector for the outgoing hadron region. The performance of this system during the test run met our expectations. The compact readout scheme based on SiPM readout works well for the HCal prototype. For the EM sections, improvements in the uniformity of light collection have to be made in the near future. With the light yield measured in the test run, introduction of properly designed masks between scintillation fibers and light guides should improve its non-uniformity. Bench test measurements with existing prototypes, as well as final data analysis and MC simulation of the exact test beam configuration, will start soon or is already in progress.

PHENIX Team Progress Report

Reporting Period: From 12/13/2013 to 06/27/2014

Project Name: EIC Calorimeter R&D at BNL

Project Leader: Craig Woody

Date: June 27, 2014

Past

What was planned for this quarter?

The main goal for the first half of 2014 was to test our tungsten scintillating fiber prototype calorimeter.

What was achieved?

The construction of our prototype tungsten plate – scintillating fiber calorimeter was completed in early January of 2014. It consisted of a stack of 1 mm tungsten absorber plates (made of two 0.5 mm plates glued together) with a layer of 1 mm scintillating fibers in between. It was designed to have the absorber plates oriented at a slight angle with respect to the incoming beam particle in a tilted plate configuration in order to allow the readout to be placed at the back of the absorber stack and to prevent channeling of particles along the scintillator. The readout consisted of an array of 7x7 towers (each approximately 2.5 x 2.5 cm) that were read out with silicon photomultipliers (SiPMs). More details of the construction of the prototype are given in our previous progress report (Dec 2013). Figure 1 shows the completed prototype calorimeter mounted in its rotation stand that was used study it in the test beam.

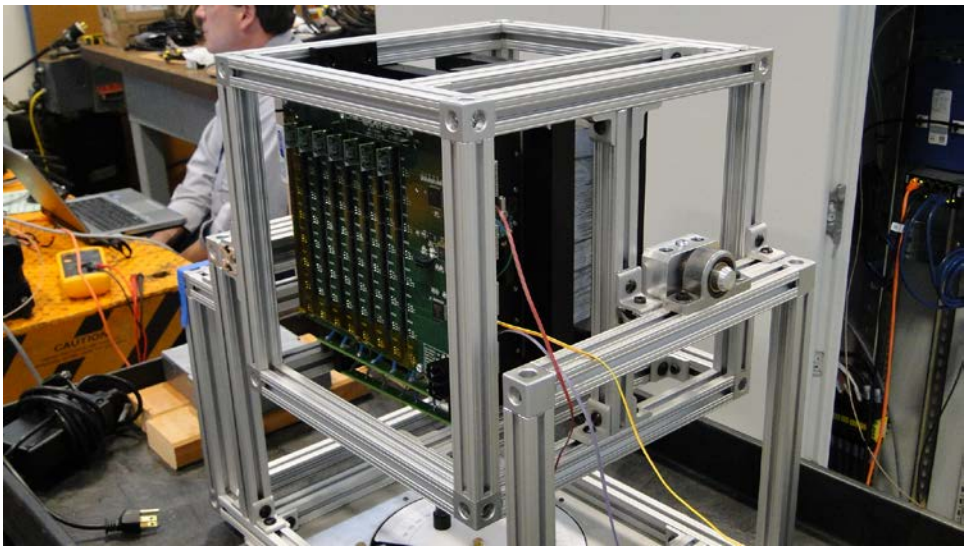

Fig. 1. Prototype tungsten plate/scintillating fiber calorimeter

The calorimeter was tested at the Fermilab Test Beam Facility in the MT6.2 test beam area in February of 2014. A prototype of the sPHENIX hadron calorimeter, which is also a tilted plate design, was also tested at the same time. Figure 2 shows the layout of the two detectors in the test beam. The EMCAL was mounted on rails such that the distance between the EMCAL and HCAL could be varied. This allowed studying various configurations the two calorimeters could have in sPHENIX.

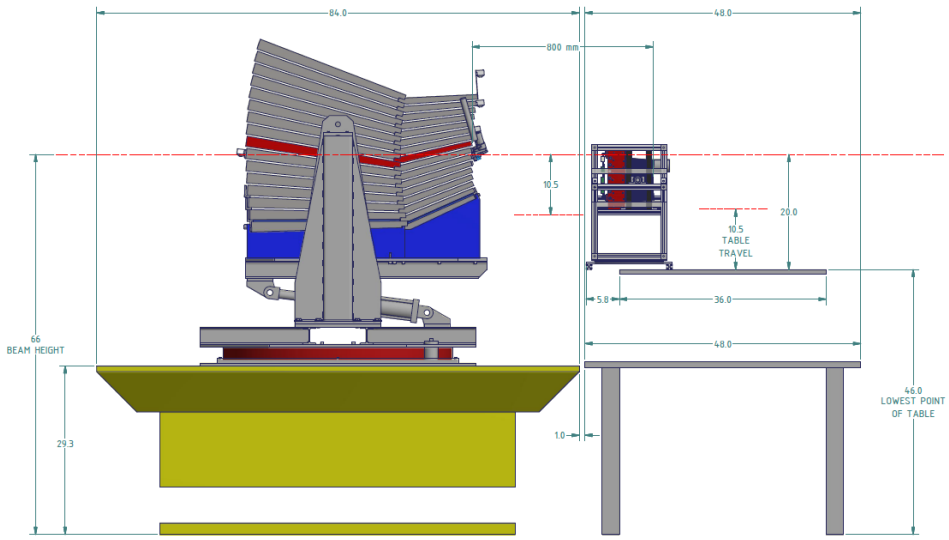

Fig. 2. Layout of the EMCAL and HCAL prototypes in the test beam at Fermilab.

The Test Beam Facility delivered beams of hadrons and electrons with momenta from 1 GeV/c up to 120 GeV/c. The 120 GeV/C beam was derived from the primary beam from the Fermilab Main Injector and was essentially purely protons, while a lower momenta, the beam consisted of a mixture of pions, electrons and muons. At lower momenta, the beam was mostly electrons, and at higher momenta, the beam was mostly pions. A Cherenkov detector upstream allowed for the identification of electrons and pions from 1 GeV/c up to 32 GeV/c. Unfortunately, it was necessary to place our two prototype calorimeters at the far downstream end of the beam line due to the rigging requirements needed to install the hadron calorimeter in the test beam area. This resulted in having a large amount of material upstream of the calorimeters in the form of beam line instrumentation, air and other material, which significantly degraded the quality of the electron beam, particularly at low momenta. It also affected the size and position of the beam at the far downstream location. A small XY scintillation hodoscope (which was lent to us courtesy of the UCLA Group) allowed measuring the beam particle position in both X and Y with a precision of 5 mm in each direction. It also served as a trigger in close proximity to both calorimeters which could be placed in coincidence with other beam line counters.

Each tower of the detector was calibrated using the MIP peak from the 120 GeV proton beam. Figure 3 shows the spectra for all of the 49 towers. These were used to equalize the response of each tower to ~ 3-4%. Unfortunately, while we had implemented temperature compensation for the gain drift of the SiPMs in our readout electronics, time did not permit us to actually use this feature during the test beam run. This would not have been a major problem if the detector had been left in one position for the entire test, but in order to test various positions and orientations, the detector was moved or reposition

frequently, which caused the heat load to change at the location of the SiPMs. Therefore, the calibration that was established with the scan of the 120 GeV beam was not necessarily stable over time, and therefore we did not have the best calibration for some of the subsequent test runs with electrons where we attempted to measure the energy resolution.

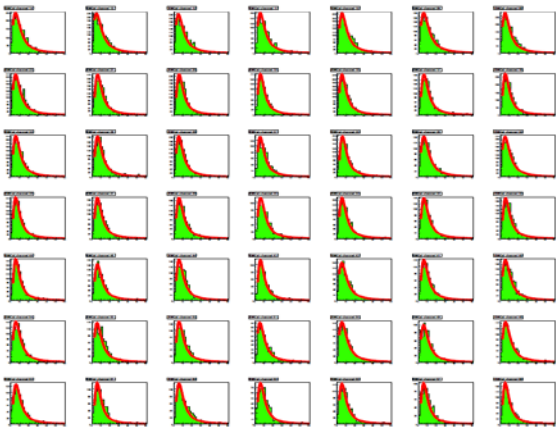

Fig. 3. MIP spectra for all 49 towers of the detector obtained with the 120 GeV proton beam.

One of the most important parameters of the calorimeter design is the light yield. In order to determine this accurately, we coupled a calibrated conventional PMT directly to the absorber stack and measured the light yield in terms of the number of photoelectrons per MeV of energy deposited in a single tower module using the 120 GeV proton beam. A minimum ionizing particle leaves ~ 29 MeV in a single tower and produces a clear minimum ionizing peak as shown in Fig. 4. Using the known phototube calibration and assuming 90% light collection efficiency in this direct coupled configuration, we infer a light yield of 3900 p.e./GeV for the absorber stack. We measured independently an average light collection efficiency of 4.7% for an individual tower with a single SiPM, which would imply a light yield of 180 p.e./MeV for a single tower with the SiPM readout. This gives a contribution ~ 7%/√E to the stochastic term in the overall calorimeter energy resolution, which is small compared to the expected resolution of ~ 12-13%/√E. Note also that adding additional SiPMs to the readout tower increases the light yield roughly in proportion to the number of SiPMs used.

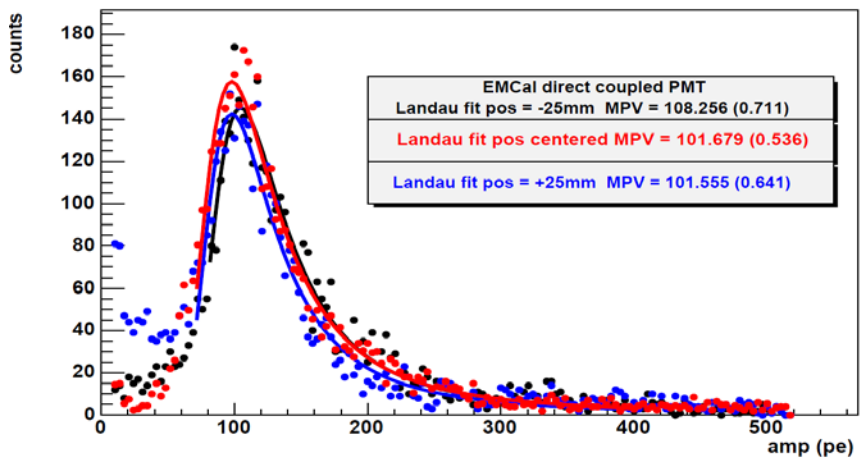

Fig. 4. MIP spectrum for a single tower module measured in several locations with a calibrated photomultiplier tube.

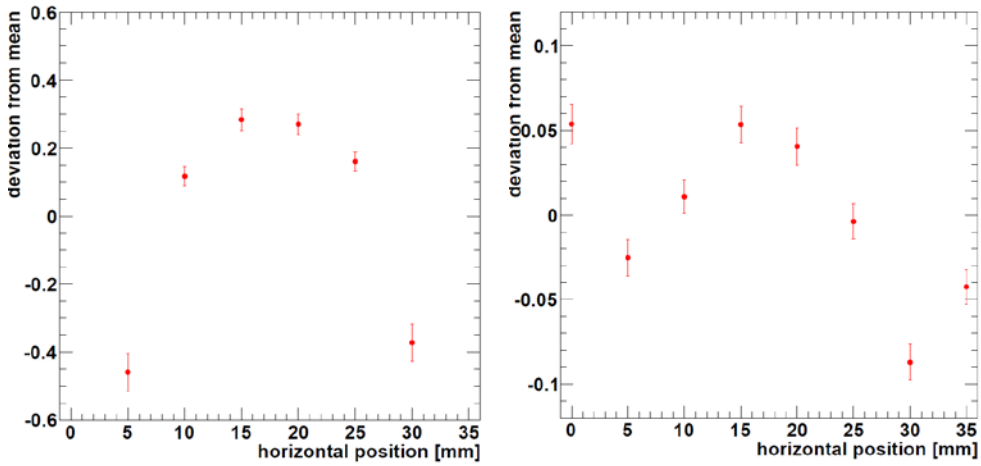

Fig. 5. Uniformity in the horizontal direction for a single row of seven towers and the sum of three rows of seven towers.

The detector was scanned in both the horizontal and vertical directions in order to measure its uniformity. The scans were done using the 120 GeV beam with the calorimeter facing downward such that the beam passed through seven towers at a time which were summed. The horizontal scan was performed using the scintillation hodoscope that allowed us measure the calorimeter response in 5 mm steps. Fig 5a shows the response of a single row of towers which shows the expected falloff towards the edges. Figure 5b shows the sum of three neighbouring tower rows which shows the much improved uniformity (note the difference in the vertical scales). The rms deviation for the sum of 3 towers is ~ 5%.

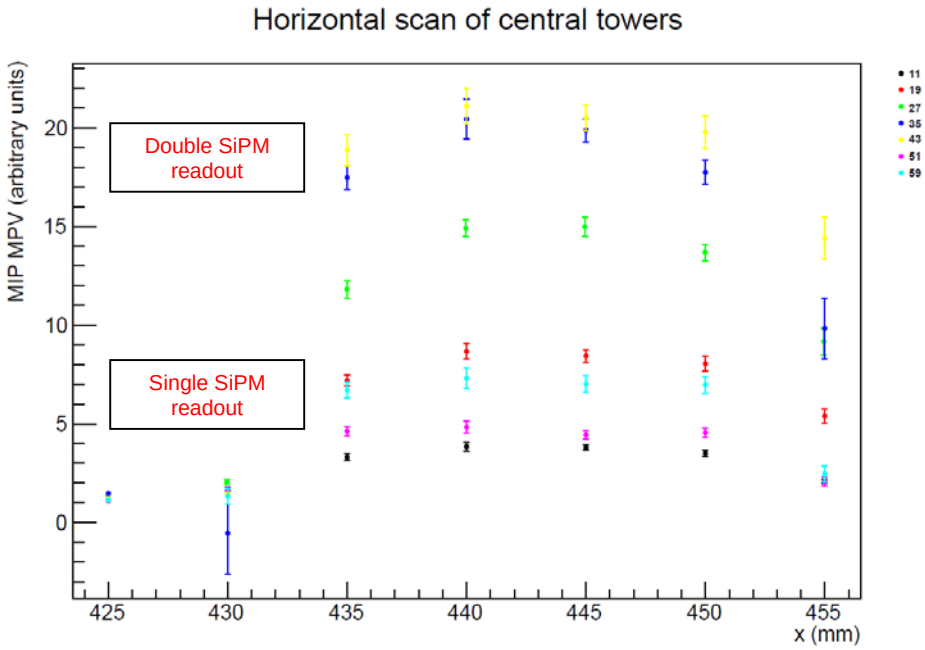

Fig. 6. Horizontal scan across rows of seven towers summed with some rows having double SiPMs readouts.

We also tested a configuration where several rows of towers had two SiPMs reading out each tower. Figure 6 shows a horizontal scan in this configuration which shows that the light output essentially doubles when two SiPMs are used.

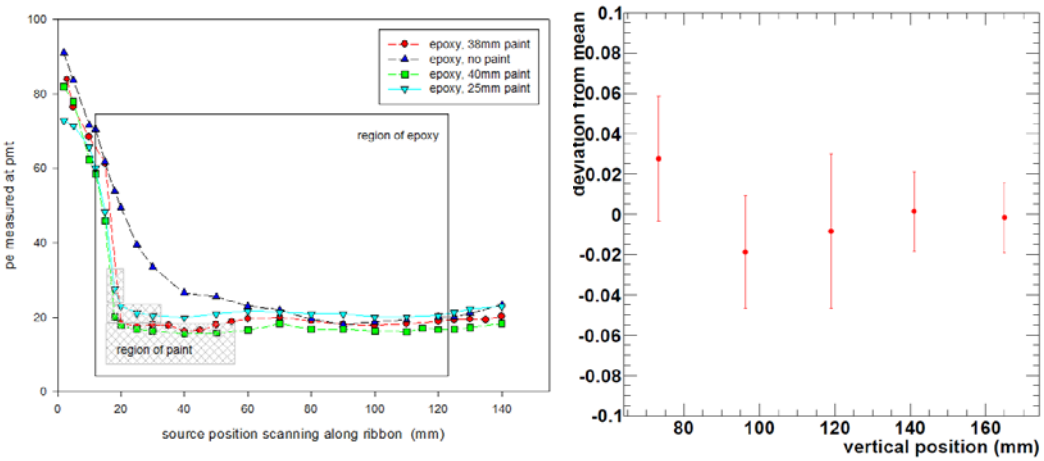

Fig. 7. Uniformity in the vertical direction for a row of seven towers.

Figure 7 shows the uniformity for a scan in the vertical direction. This measured the longitudinal response of the calorimeter, which effectively studied the longitudinal light output uniformity of the fibers. The fibers were painted with black paint at the readout end in order to make their response flat, as shown in Fig. 7a. The resulting uniformity is shown in Fig. 7b, which gives an rms deviation of ~ 2%.

What was not achieved, why not, and what will be done to correct?

Unfortunately, we were not able to obtain a reliable measure of the energy resolution due to the temperature variation of the SiPMs that we were not able to compensate for. This was complicated by the fact that the detector was moved or repositioned frequently which changed the heat load on the SiPMs and caused gain instability. We are currently looking at ways of correcting for this in the data analysis using the LED monitoring system and the known temperature dependence of the SiPMs and we hope to be able to eventually extract the energy resolution from our current data set.

Future Plans for both the RD1 Team and the BNL PHENIX Team

What is planned for the next quarter and beyond? How, if at all, is this planning different from the original plan?

- With the second successful test of the tungsten SPACAL and the adoption of this technology for both the PHENIX and STAR future upgrades, we now plan to develop a cost effective means for mass production of these calorimeter modules in various forms (e.g., non-projective for the STAR FCS, projective in ϕ for an EIC barrel calorimeter, and to study the possibility of producing modules that are projective in both ϕ and η). We also plan to develop a detailed mechanical design that could be used to support groups of modules, and eventually build a full scale prototype that can be tested both mechanically and in the test beam.

- We will also investigate improving the energy resolution of the SPACAL by increasing the sampling fraction by adding more fibers to the matrix. We believe we can improved the energy resolution to ~ 5%/√E using the procedure. However, we will have to investigate the mechanical properties and assembly procedure, light output, uniformity, and energy resolution of the resulting modules.
- We will try and improved the light collection uniformity of the SPACAL towers by introducing an optical mask to compensate for the residual non-uniformity in the current tower design. We feel we have sufficient light output to do this and that it will not compromise the final energy resolution.
- We plan to continue our development of the readout electronics for the SPACAL and forward HCAL. This is presently being carried out by two groups, one at BNL and the other at Indiana University. While they are somewhat different in their approach, both include the essential features of gain equalization and temperature compensation for the SiPMs
- Since SiPMs are used extensively in virtually all EIC calorimeter applications, we plan to investigate radiation damage in SiPMs as a part of our study. We have already been in contact with several groups that are carrying out studies on radiation damage in SiPMs (CMS, Gluex and DESY) and will utilize their experience and data to try and estimate the effects on these devices at EIC and will certainly continue to follow these developments. However, we will also carry out our own radiation damage studies with neutrons using the Indiana University Cyclotron Facility Low Energy Neutron Source (LENS), and with gamma rays and hadron irradiations at BNL. In addition, both STAR and PHENIX have made measurements of the neutron and ionizing radiation levels in their respective IRs which will be used to provide input for simulation studies.
- Simulation studies will be needed to estimate the radiation levels that will be expected for any EIC detector, and it will consist of several parts. One will be to try and estimate the level of synchrotron radiation produced by the machine in the region of the IR. These simulations are currently being carried out by the Collider Accelerator Department and we will use this information when it becomes available. In addition, we will need to estimate the neutron and ionizing radiation levels in the IR, which will require a separate simulation that includes the detailed geometry of the IR and all of the detectors and surrounding materials inside. STAR has already carried out some preliminary calculations and made estimates of the neutron levels in their IR, and we plan to build on their experience to develop a more detailed simulation for an EIC detector.

What are critical issues?

- Develop mass production techniques for constructing SPACAL modules
- Develop a mechanical design for supporting groups of modules and design a full scale prototype for the SPACAL
- Complete the design of the front end electronics and readout systems for SPACAL and forward HCAL
- Improve light collection uniformity of individual towers of SPACAL
- Measure neutron, gamma ray and hadron damage in SiPMs
- Carry out simulations to estimate neutron and ionizing radiation levels for an EIC detector and its IR

Budget:

We are not requesting any additional funds for work on the tungsten EMCAL or forward HCAL for the second half of FY 2014. However, we expect to request additional funding on the order of 150k to continue the efforts from both RD1 team and the BNL PHENIX team on the R&D for EMCal detectors in FY2015.

Crystal R&D Project

BSO Crystal R&D Progress Report by the USTC Team
Reporting Period: From 01/2014 To 06/2014

Project Name: Crystal R&D for a Forward Calorimeter at EIC

Project Leader: Yifei Zhang

Date: 25/06/2014

The planned work and the progress for the report period:

1) BSO R&D status and the performance.

The light yield output (LY) of the BSO crystals produced last year is about a factor of 4 higher than that of PWO crystals in room temperature and similar as PWO 's LY in -25°C as in previous reports.

Beyond this there is no much improvement of BSO production from SICCAS. Recently SICCAS just produced two new BSO crystals and will deliver to us by this week (around June 28th). We will test them to see if there is any improvement.

The 3x3 prototype will be completed with the two new crystals and we will test the prototype again for the performance study before the beam test. The beam test is scheduled at CERN in this November.

One of the critical issue is the longer decay time of BSO, ~100ns. However, from simulation, we found this is not a problem, since the track occupancy in the electron direction ($-4<\eta<-2$) is very low. Left figure below shows the pseudo-rapidity distributions for electrons (red) and hadrons (blue) from 1 million e+p events at 5+250 GeV. There are only 0.4 tracks per event in $-4<\eta<-2$. Assuming the BSO EMC is located at -145cm alone the beam line, the total number of crystals in this kinematics region will be ~1240, see the right figure below. If the e+p collision rate is ~10M/Hz, in the integration time of 600 ns, within which the most of the LY will be integrated, the track occupancy can be roughly calculated as 0.002 per channel or 5×10^{-4} cm^{-2}.

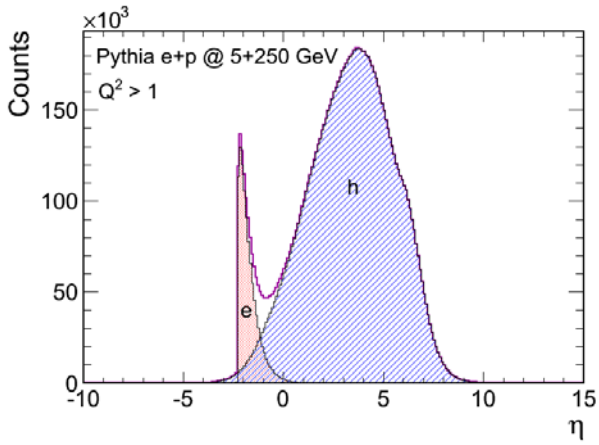

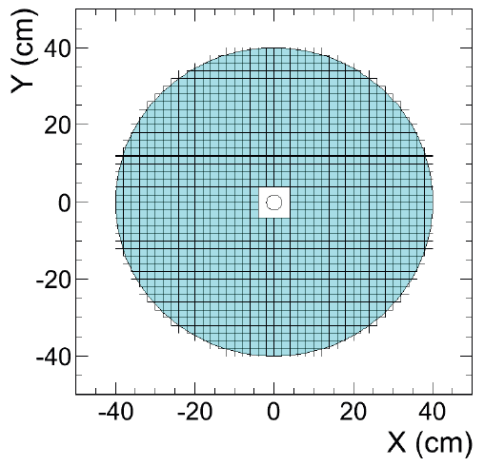

2) Beam test for the BSO prototype.

There is no beam test yet so far since the beam test is scheduled at CERN for about two weeks in the beginning of this November.

Future

1) Test new BSO crystals produced from SICCAS, send feedback to them and discussion on the BSO production development.

2) Test the prototype with completely assembled 3x3 crystals before the beam test.

3) Beam test at CERN and summarize the test results compared to simulation.

New Proposal

Project Name: Crystal Calorimeter Development for EIC based on PbWO4

Project Leader: T. Horn

Date: 27/06/2014

Team Members:

T. Horn[1,4], C.Munoz-Camacho[2], H. Mkrtychyan[3],R-Y. Zhu[5], C.Woody[6]

1) The Catholic University of America, Washington, DC 20064
2) IPN Orsay, France
3) Yerevan Physics Institute
4) Thomas Jefferson National Accelerator Facility, Newport News, VA 23606
5) California Institute of Technology, Pasadena, CA
6) Brookhaven National Laboratory, Upton, NY

Abstract

An important requirement for the EIC endcap electromagnetic calorimeter is high-resolution in the electron going direction in order to measure the energy of the scattered electron with high precision. The calorimeter should provide angular resolution to at least 1 degree to distinguish between clusters, have an energy resolution ~ few %/√E for measurements of the cluster energy, and withstand radiation to at least 1 degree with respect to the beam line [1,2]. Crystal calorimeters have been used in nuclear and high energy physics for their high resolution and detection efficiency and thus would be the preferable solution for the future EIC. In particular, a solution based on $PbWO_4$ would be optimal due to its small Moliere radius and radiation hardness. $PbWO_4$ has been used for existing calorimeters (CMS, JLab Hall B) and high quality crystals are being considered to be used in several new electromagnetic calorimeter projects around the world (PANDA, JLab 12 GeV). The critical aspect for crystal quality, and thus resolution, is the combination of high light output and radiation hardness, which depend strongly on the manufacturing process. During the CMS ECAL and early PANDA EMC construction, two manufacturers, BTCP and SIC, using different crystal growth methods were available. Basically all high quality crystals have been produced at BTCP using the Czochralski growing method, whereas SIC produces crystals using the Bridgman method. BTCP is now out of business, and the worldwide availability of high quality $PbWO_4$ production has changed dramatically. Recent studies of crystals from SIC, the remaining manufacturer of crystals, seem to indicate major problems maintaining good crystal quality. It is therefore not clear if crystals of the same quality as those produced by BTCP are in fact currently available. Based on this current situation, there is a clear need to develop an alternate supplier of $PbWO_4$ if it is to be used for a future EIC crystal calorimeter in parallel with the current efforts.

The main goal addressed by the proposed R&D is to identify what would need to be done to be able to build a $PbWO_4$-based endcap calorimeter for the EIC exploring the limits of $PbWO_4$ quality. Such an R&D effort fits naturally into the global EIC calorimeter R&D program and could also have an impact on the worldwide $PbWO_4$-based electromagnetic calorimeter construction.

1. Introduction

The primary goal of the EIC Calorimeter Consortium is to explore and develop the technologies for the calorimetric measurements that will be required for future experiments at the Electron Ion Collider. Both electromagnetic and hadronic calorimeters will be required to perform the critical physics measurements at EIC over a large kinematic range. These physics measurements are described on the EIC Wiki page [3] and in our original proposal [4], and there has been an ongoing effort by the EIC Calorimeter Consortium to address these needs over the past two years. Much of that effort, due mainly to the scale and complexity of the systems involved, has been devoted to the barrel calorimeter region, covering the rapidity range from $-1 < \eta < 1$, where the requirements on the energy resolution for the electromagnetic calorimeter is ~ 12%/√E. However, in the electron going direction, it will be necessary to measure the scattered electron with much higher energy precision, to have good position resolution, and to be able to survive much higher radiation levels than in the central region.

The PID requirements are primarily driven by semi-inclusive and exclusive processes requiring good resolution in angle to at least 1 degree to distinguish between clusters, energy resolution to a few %/√E for measurements of the cluster energy, and the ability to withstand radiation down to at least 1 degree with respect to the beam line [1,2]. A $PbWO_4$-based calorimeter would be an optimal choice, having a small Moliere radius and also providing excellent energy resolution. An example of this is shown in Fig. 1, which shows that the HYCAL calorimeter at JLab [5] yielded an energy resolution of $\sigma/E=1.3$ % and a coordinate resolution of σ_x ~1.28-2.10 mm at a neutral pion energy of 5 GeV, giving an invariant mass distribution with a width of 2.3 MeV/c^2.

When selecting a neutral particle detection system, it is also important to pay attention to the effect of radiation dose on the performance of the spectrometer. In particular, attention must be paid to degradation of the crystal optical properties and recovery thereof, and damage to the photo-sensors. The background rates could also directly affect the resolution of the spectrometer. A crystal-based calorimeter with crystals of high radiation hardness and high light output for good energy resolution is thus the best option to detect photons from DVCS or π^0 decay and scattered electrons, and virtually all EIC detector proposals [1,2,6,7,8,9] intend to use a crystal calorimeter in the forward electron going direction.

Crystal detectors have been used widely in high energy and nuclear physics experiments, where total absorption electromagnetic calorimeters made of inorganic crystals have been employed for decades because of their excellent energy resolution and detection efficiency for photon and electron measurements. Crystal electromagnetic calorimetry is the choice for experiments where precision measurements of photons and electrons are essential. $PbWO_4$ has been used at hadron colliders (CMS/ECAL) and at electron accelerators (JLab Hall B/HYCAL). Because of its resolution, timing, and also its radiation hardness, it will also be used at PANDA/EMC and at JLab 12 GeV (NPS, HYCAL, Hall B). $PbWO_4$ crystals are fast (5-14 ns) and therefore suitable for these experiments, which require fast signals with short decay times to minimize pile-up at high rates, providing a resolving time resolution of better than 100 ns. Also important are crystal geometry and integrity. A comparison of $PbWO_4$ with some other dense crystals is given in Table 1. LSO/LYSO is a crystal with acceptable timing, but at the present time, is very expensive (~ \$50/cm^3). Our consortium currently has an ongoing effort to explore the use of BSO, which has a slower decay time (~ 100 ns), but could provide a more cost effective option for a forward electromagnetic calorimeter. However, this crystal is still in the early stages of development, and the true production costs and quality issues with mass production of this material are not really known. Other

candidate crystals for the EIC endcap calorimeter could be BaF_2 and PbF_2. Though we may explore some of them, a full investigation of these alternative crystals is outside the scope of this first year R&D proposal and we defer such studies to subsequent years.

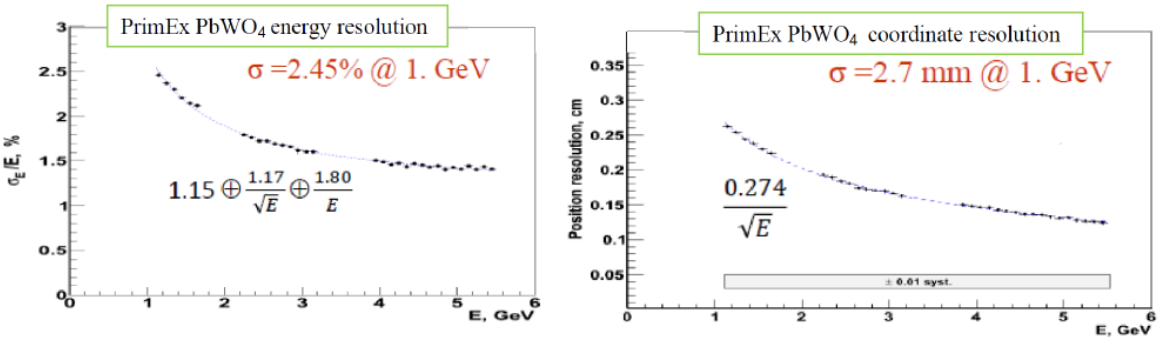

Figure 1. The energy and position resolutions of $PbWO_4$ crystals from the HYCAL at JLAB [5].

Parameter	Lead Tungsten (PbWO4)	Lead Fluoride (PbF2)	Bismuth Germanate (BGO)	Luterium-Yttriu (LSO/LYSO)
Density (g/cm³)	8.28	7.66-7.77	7.13	7.2-7.4
Rad. length (cm)	0.89	0.93-0.95	1.10-1.12	1.16
Refractive index	2.20	1.82	2.15	1.82
Emission peak (nm)	420	~310, ~280	480	420
Moliere radius (cm)	2.19	2.22	2.15	2.07
Radiation type	Scint. (~13% Č)	Pure Čer.	Scint. (~1.6% Č)	Scintillation
Timing property τ (ns, %)	5 (73%); 14 (23%); 110 (4%)	Fast, <30	300	40-50
Effective Z	73	77	83	65
Hydroscopicity	No	No	No	No
Interact. Length (cm)	~20.7	~21	~22.7	~20.9
Rad, hardness (krad)	~20-50	~50	~1,000	>1,000
Light yield LY (photon/MeV)	~140-200	~2-6	~5,000-10,000	~5,000-30,000
d(LY)/dT (%/°C)	-2.0-2.5	No	-0.9	-0.2
Critical energy (MeV)	~9.6	8.6-9.0	7.0	9.6

Table 1: Comparison of the properties of various dense crystals

2. Growth and Production of $PbWO_4$ crystals

Mass production of PbWO4 was developed by CMS in order to produce the 76k crystals required for use at LHC. However, the requirement on the light output of these crystals was moderate, since the expected energy range for the Higgs search was beyond 100 GeV. The crystals for CMS were commercially available from the two manufacturers: BTCP in Russia and the Shanghai Institute of Ceramics (SIC) in China. BTCP produced crystals using the Czochralski method, while SIC uses the Bridgeman method. Groups at PANDA started efforts to extend the application of $PbWO_4$ down to energies of a few MeV for photon detection in low and medium energy physics. In collaboration with BTCP, a significant improvement in light output and radiation hardness was found.

To grow the crystals tungsten oxide (WO_3) and lead oxide (PbO) powders of purity 99.99% were used as the initial materials. The best quality $PbWO_4$ was grown

from a 50%–50% mixture of PbO and WO_3 which melts congruently at 1123°C, without a phase transition during cooling. Later analyses revealed that crystals with poor radiation hardness have a non-optimal Pb/W ratio. The standard method to grow $PbWO_4$ crystals is the Czochralski method. This method was used in Russia and the Czech Republic. Raw materials (a mixture of PbO and WO_3) were first melted in a platinum crucible from which up to three ingots of 2 kg of polycrystalline $PbWO_4$ were grown. This polycrystalline $PbWO_4$ was then used as starting material for crystal growth in a second stage. During the second stage, the crystal was doped with La, Lu, Gd, Nb or Y at concentrations from few tens of ppm to ~100-200 ppm. The best timing and light yield were achieved with combined double doping La and Y ions at the level of < 20 - 100 ppm, or triple doping of Mo, Cd and Sb. SIC crystals are doped with only yttrium. The original PWO for CMS required a strong doping to compensate defects. The new development by the PANDA group in collaboration with BTCP significantly improved the concentration of defects on the level of at least a factor two, reducing the doping concentration and increasing the light output by almost a factor of two. This material is called PWO-II. In addition, $PbWO_4$ can be operated at low temperatures. When operated at -25°C as at PANDA, the light output is increased by almost a factor of 4, while still being able to collect > 90% of the light within 100 ns.

Gamma-ray induced radiation damage in $PbWO_4$ is well understood. The scintillation mechanism in $PbWO_4$ is not affected. The damage is caused by radiation induced absorption, or color center formation. The damage recovers under room temperature, leading to a dose rate dependent damage level because of the balance between color center formation and annihilation [10]. It is also believed that radiation damage in $PbWO_4$ is caused by oxygen vacancy which is lattice structure related defects [10]. In terms of radiation damage, operation at low temperature blocks most of the statistical and thermal annealing processes and accumulates the population of color centers up to the intrinsic defect density. It is well known $PbWO_4$ crystals can be thermally annealed or optically bleached, e.g., by illumination with blue or even near infrared light. If the photo sensors are blind to infrared light, illumination could be performed continuously as considered for the forward endcap of PANDA-EMC.

Radiation hardness and recovery of the crystals also depend on the type and concentration of doping material. After ~50-100 krad accumulated dose for about one month out of beam, the La-doped crystals will almost completely recover, whereas Nb-doped crystals will only recover 30% to 40% of the initial damage. Note that all of the characteristics above are dependent on the exact production technology and may vary from company-to-company, or even within the same company from batch-to-batch. One should thus carefully study the product quality (light yield, timing, radiation hardness and UV recovery) and do adequate prototyping before one can procure the full quantity of the required crystals for any detector. It is also important to know if the company will perform quality control measurements and be willing to invest in R&D efforts before delivery to be sure that all parameters of the crystals are within the required limits.

Based on recent experience with almost 10000 $PbWO_4$ crystals from BTCP, one can get a relatively narrow distribution of most of the essential parameters like light yield, optical transparency, etc. In the case of the radiation hardness, there is no real correlation with any of the other parameters. It is a question of raw material and the production process. Some crystals obtained by PANDA proved to be extremely radiation hard, but with a reduction of the absorption coefficient even below 0.3 m^{-1} imposing an integral dose of gamma rays (^{60}Co) of 30Gy within an irradiation period of about 10 minutes. However, it did demonstrate that it is indeed possible to obtain very radiation resistant crystals. The critical requirement is to obtain *high light output combined with radiation hardness*, and thus the defect concentration has to be kept low.

Recent studies of crystals from SIC show that there are major problems with maintaining good quality control. All distributions of any quality parameter were found to be much wider than the results for the BTCP crystals. Fig. 2 illustrates the longitudinal transmission for five $PbWO_4$ samples from SIC as a function of wavelength, not

corrected for Fresnel losses due to reflection, in comparison to the typical transmission curve of crystals produced at BTCP. While it is known that the longitudinal transmittance of BTCP crystals is generally better than that of SIC crystals because of the birefringence nature of PWO and the different crystal growth axis for these two technologies as discussed in Ref. [11], in particular, in the UV region, the results in Fig. 2 show a relatively poor consistency in transmittance among the SIC crystal samples analyzed. These problems might be caused by the Bridgeman technology or details of the manufacturing process at SIC. Therefore, if one needs crystals of very good optical quality, a better approach might be to follow the details of the manufacturing process previously used by BCTP. This process is also used by the company Crytur [12] in the Czech Republic, which we intend to involve in this R&D.

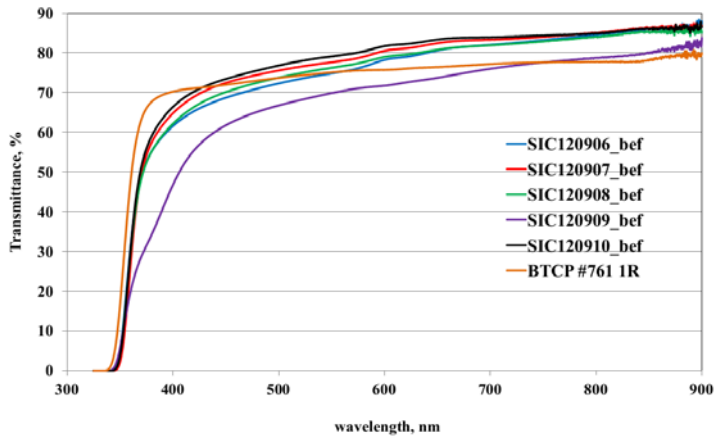

Figure 2. The optical transmission of the 5 $PbWO_4$ samples measured before irradiation in comparison to a typical BTCP crystal.

They not only use the Czochralski method for growing crystals, they also have access to the same raw material (i.e., powder) that was used by BCTP including sensible details on the growing process. It would therefore seem likely that they should be able to produce crystals of the same quality and radiation hardness as BCTP did for CMS and within a tolerable time period. However, they do not have the actual furnaces that would be required to produce crystals of the size, shape and number that would be needed for an actual calorimeter. Supplying them with some initial funding to invest in these facilities and to start producing crystals of the size and shape we require is one of the main purposes of this R&D.

3. Proposed R&D

3.1 General Goals

The main goal of the proposed R&D is to investigate the limits of PbWO4 crystal quality to see what needs to be done if $PbWO_4$ was to be used in future EIC detector. Superior quality is particularly important in regions where high doses are expected. The goal is not to complete a detailed design of the endcap calorimeter for the EIC, but to address key issues through simulations, prototyping, and tests, and to establish the level of performance that could be reached in at least one configuration with $PbWO_4$. The R&D activity proposed here could also be considered as a common effort together with PANDA and JLab/NPS. In case of PANDA, more than 8000 crystals are still missing due

to the unfortunate close down of BTCP. Such a collaboration would provide mutual benefits in the evaluation of the $PbWO_4$ crystal quality, and would enable producing crystals again using the same procedure and raw material that has already proven to provide high quality crystals. Working in close collaboration with Crytur to develop high quality crystals will be important to ensure that crystals will be produced to the required specifications. Crytur is currently the only manufacturer willing to start $PbWO_4$ production using the Czochralski method, and developing a $PbWO_4$ crystal of high quality that can be produced in large quantities by a vendor would be of interest to a broad community.

3.2 Simulation Studies

At the present time, there is no detailed or accurate estimate of the radiation dose that is to be expected for the forwards crystal endcap calorimeter at EIC. There are estimates of particle production over a wide range of rapidity, which can be found on the EIC Wiki page [13] and these rates can be used to estimate the energy deposit (and hence the dose) from charged and neutral particles (photons, neutrons and K^0_L's) produced by beam interactions. However, there is no current estimate on the dose from synchrotron radiation produced by the electron beam, nor from secondary particles produced in the beam pipe, magnets, detectors or surrounding material, and these processes are probably the largest contributors to the total dose seen by the forward crystal endcap calorimeter. Simulation calculations of the synchrotron radiation dose are currently under way by the JLab [6] and BNL Collider Accelerator Departments, and we will use those rates to estimate the expected dose for the crystals when they become available. However, the dose rates for secondary particles is much harder to estimate, since it requires a detailed model of the interaction region, including the beam line, magnets, detectors and surrounding structures. We plan to be able to model this to some level and make some preliminary estimates of the dose, but we expect that this will be an ongoing effort to continuously refine these estimates as the model of the detector and IR evolves.

3.2 Evaluation of Crystal Quality

We will test the performance of $PbWO_4$ crystals, and in particular, measure their light yield, optical transmission, uniformity and radiation hardness. The combination of high light yield and good radiation hardness is the defining characteristic of a high quality crystal. To explore the limits of crystal quality, we propose to obtain a set of $PbWO_4$ crystals from Crytur that are manufactured using the Czochralski method and raw materials from which high quality crystals have been grown at BTCP. For an initial comparison, we will use the $PbWO_4$ crystals from SIC that were already procured by JLab for the Hall C Neutral Particle Spectrometer (NPS) project. A comparison to the older HYCAL crystal, as well as PbF_2 from the Hall A DVCS experiment, may be possible as well. However, care must be taken when comparing older SIC crystals produced some time ago since as mentioned before the raw material *and* details of the production process are important. Both of these may have changed over the last few years. Recently received SIC crystals seem to exhibit major deficiencies in quality even when grown with raw materials used at BTCP. The best way to compare SIC crystal quality would thus be with a set of crystals produced to specifications and known details of the production process. A budget for such SIC crystals is given in Table 3.

The homogeneity of the crystal could be investigated based on the variation of the transverse optical transmission. A quality parameter that characterized the band edge absorption of the crystal can be defined as the maximum variation of the wavelength at a transmission value of T=50% along the length of the crystal. In addition, the quantity δ, which is the maximum % deviation of the transverse transmission from the value measured at the center, can also be used. Therefore, the transverse optical absorbance of all crystals, as well as their longitudinal transmission, will be measured as

function of wavelength in order to fully characterize their quality.

The crystal optical transmittance will be measured using the existing setup at JLAB, shown in Fig. 3, that is also being used for tests for the NPS. Additional tests could be done at CUA with a Perkin/Elmer photospectrometer investigating a range of wavelengths between 250 and 900 nm. In addition, there are extensive facilities for characterizing a wide variety of crystals at Caltech [14] and in the BNL Physics Department. These groups also have extensive experience and expertise in performing these kinds of measurements.

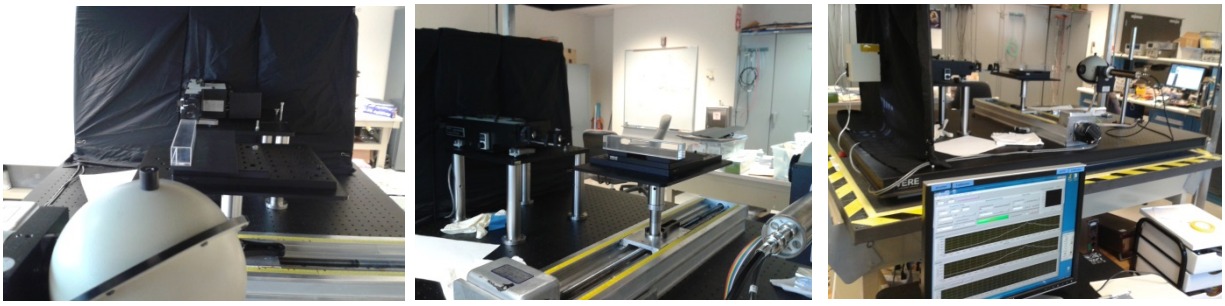

Figure 3. Setup for measuring transmission and light output of $PbWO_4$ crystals from the HYCALat JLAB.

To improve the light collection from the crystals, we will study a variety of reflective materials, for instance VM2000, and Tedlar as used for the HYCAL and PANDA. In the initial phase, the crystals will be attached to photomultiplier tubes like the Hamamatsu R4125 used in the NPS prototype. Since the $PbWO_4$ light yield is temperature sensitive the crystals would be measured in a temperature controlled enclosure. The light yield could be measured using a ^{137}Cs source emitting photons of 662 keV and calibrated in terms of photoelectrons.

We also intend to study of the light output of the various $PbWO_4$ crystals using silicon photomultipliers (SiPMs). These would be ideal photo sensors for reading out the crystals since they produce high gain (~ $3x10^5$) and work inside a magnetic field, given that the EIC forward endcap calorimeter would sit inside the fringe field of a solenoid magnet. Our consortium has gained a great deal of experience with SiPMs in the R&D work that it has done for the barrel calorimeters, including developing readout electronics, gain and temperature control circuitry, light collection studies, which can be easily be extended to using them for the crystals in the forward endcap. We would therefore measure the light output from the crystals using SiPMs of various types, such as the 3x3 mm^2 devices (Hamamatsu S10931-025P, or the new S12572-025P) that have been used for the sPHENIX and STAR prototype calorimeters.

One of the main issues to study will be the light collection, in which we will need to match the roughly 2x2 cm^2 area of the crystal to the much smaller are area of the photosensor. This may require some combination of using a light guide or light collection cavity along with using multiple SiPMs. Both the light collection efficiency and light collection uniformity will be measured. The overall light yield (i.e., number of photoelectrons per MeV) will also be measured.

3.3 Gamma Ray Radiation Damage Studies

The primary goal of the radiation tests is to evaluate the performance of $PbWO_4$ crystals from Crytur and compare them to crystals obtained from SICCAS. Radiation damage studies will be performed at the Caltech [14] and BNL [15] radiation facilities. Both facilities can provide gamma ray exposures using a ^{60}Co source at dose rates from a few hundred rad per hour up to a few times 10^4 rad per hour. We will study the

samples over a range of exposures, starting at ~ 1 krad and going up to ~ 10 Mrad in progressive steps (e.g,, 10^3,10^4,10^5,10^6,10^7 rad). For comparison, the DVCS experiment with the NPS at JLab (at very small/forward angles) projects integrated doses of 2-4 Mrad. Measurements will be taken before and after exposure in order to characterize the changes in optical transmission and light output at each step. Recovery from damage at room temperature, as well as thermal and optical annealing will also be studies. Similar studies have been done with numerous other crystals at these facilities. Both Caltech and BNL are well equipped to perform these measurements and have a great deal of experience in analyzing and interpreting the data. In particular, Caltech played a major role in developing the $PbWO_4$ used by CMS and has studied numerous other crystals produced at SIC. Many examples of their work can be found in the literature, e.g. Ref. [10,11,16]. As illustrated in Fig. 4, the performance of the PANDA PWO-II crystals produced at BTCP is superior to the earlier CMS $PbWO_4$ crystals thus demonstrating a level of performance that could be expected for future calorimeter applications like the EIC. However, as discussed above crystal performance depends critically on the details of the production process and raw materials. Recently produced SIC crystals have shown major deficiencies, which could be related to the production method. It is thus extremely important to evaluate what would need to be done to obtain high quality $PbWO_4$ crystals.

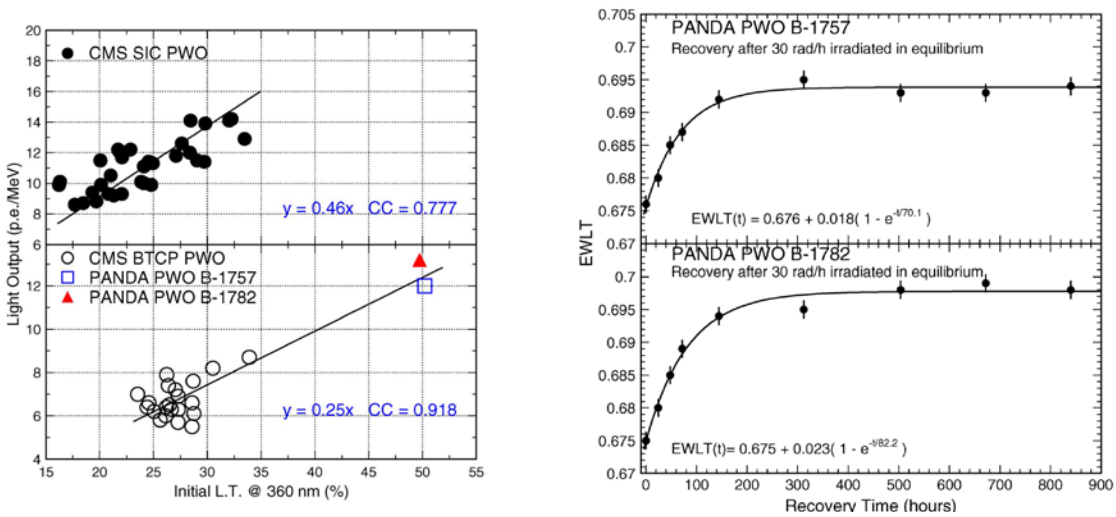

Figure 4: ***Left:*** Correlations between the initial light output (y) and the initial longitudinal transmittance (x) at 360 nm. ***Right:*** Recovery of the PbWO4 emission weighted longitudinal transmittance (EWLT) irradiated at 30 rad/h. The EWLT is a direct measure of the transparency of the crystal's scintillation light. The initial EWLT values of about 70% were not reached after 900 hours recovery indicating deep color centers inside the crystal samples [16].

3.4 Hadron Damage Studies

In addition to damage causes by ionizing radiation, damage in crystals can also be caused by high energy charged particles and neutrons [17,18]. Such studies require the use of particle beams, and the NASA Space Radiation Laboratory at BNL [19] can provide beams that can be used for these types of measurements. This facility can deliver proton beams with kinetic energies from ~ 50 MeV to 2.5 GeV at rates of up to 10^{12} p/spill, with one spill typically every 4 seconds. The beam spot can be made as small as ~ 1 cm, or can be spread out over a larger area. With these rates, it should be possible to achieve a total dose ~ 10 Mrad in $PbWO_4$ crystals in roughly half an hour. However, lower dose rates are certainly possible and would be more appropriate for

these studies. In addition, other types of crystals, such as BaF_2, PbF_2, CsI and LSO/LYSO will be studied for comparison.

We plan to expose several crystals from Crytur and SIC to proton beams at the NSRL and accumulate does of up to 10 Mrad in steps starting a 1 krad, similar to those used in the gamma ray irradiation studies. Light output and transmission measurements will be made before irradiation and between each step. As in the case of gamma ray damage, recovery at room temperature and optical and thermal annealing studies will also be performed.

3.5 Neutron Damage Studies

Determination of the radiation levels and the radiation hardness of detector materials, sensors, and electronic components is an important design requirement for any EIC detector. SiPM sensors and devices such as FPGA based TDCs close to the detector need special attention. Results of previous studies have shown that both the dark count rate and the dark current of SiPMs increase linearly as a function of total neutron fluence, and the damage does not depend on the temperature or operating voltage [20]. Part of the acute damage can be recovered by increasing the temperature of the damaged device during non-irradiated periods. Damage in SiPMs due to ionizing radiation has also been measured and may be caused by a different mechanism [21]. Damage due to hadrons has also been observed and could be caused by even other effects [22].

Since it is expected that SiPMs will be used extensively in many EIC detectors, measuring and understanding damage to these devices in a radiation environment is an important issue. There is hope that the new generation of Hamamatsu SiPMs with metal resistors are more radiation hard compared to the old generation with poly silicon resistors. wWe plan to carry out some preliminary measurements with both gamma rays and hadrons with these devices to obtain some first results. In addition, neutron damage studies can also be carried out in a neutron beam at the Indiana University LENS Facility [23] or with a neutron source at BNL. An independent study of radiation tolerance of SiPMs is also being done at JLAB as a continuation of the measurements done in [20].

3.6. Construction and testing of a prototype detector

We hope to be able to complete the initial study of the quality and radiation hardness of the new $PbWO_4$ crystals produced at Crytur using the Czochralski method and the original BCTP powder during the first year of our R&D program. However, this will depend on the time scale and success in growing these crystals at Crytur, and the quality of the first samples that we measure. Assuming they are successful, in the second year of our R&D, we would build a small prototype detector consisting of a 5x5 matrix of the new improved crystals. This would allow us to study these crystals in test beam and measure the actual energy and position resolution that we could achieve with them. This beam test would most likely be done at either SLAC where one can obtain a high precision beam of electrons with a momentum up to 15 GeV or at Jefferson Lab where the upgraded CEBAF provides electron beams up to 11 GeV.

The prototype setup could be based on that for the JLab NPS, which has an active area of about 6x6 cm^2 including a crystal matrix of $PbWO_4$ (and PbF_2 to test hybrid configurations of crystals) in a copper frame. The readout is done by 19 mm Hamamatsu R4125 PMTs with a JLab developed new active HV base [24]. The prototype will test light monitoring as well as two approaches for a crystal curing system: a standard system with a blue light source and IR curing with wavelengths > 900 nm. The NPS prototype IR curing system was constructed using superbright LEDs like the OSRAM LD274 with peak wavelength 950 nm and Vishay TSAL7400 with peak wavelength 940 nm. One could consider using the NPS prototype or a modified version of it, which could provide flexibility in the construction schedule.

As a second stage of testing we propose to investigate reading out the calorimeter with SiPMs or other sensors with tolerance to radiation and magnetic fields. This would be the first time SiPMs would be used to read out this type of calorimeter. We will benefit from JLab's experience with these devices with, e.g., the GluEx project and the DIRC project, which is also funded by the EIC R&D program. We expect that we will be able to reuse many of the SiPMs from our R&D on the barrel calorimeter, and therefore will not need to purchase new SiPMs for this test. We should also be able to use much of the readout electronics and the calibration system from the small tungsten scintillator prototype calorimeter that was built as a part of that project. Most other electronics, such as amplifiers, discriminators, scalers, readout controller and DAQ, system are available at JLAB. Therefore, the main item that would need to be purchased for constructing the $PbWO_4$ prototype calorimeter would be the actual crystals for the matrix.

4. R&D Timeline and Deliverables

	Year 1 by Quarters				**Year 2 by Quarters**			
Deliverable	**Q1**	**Q2**	**Q3**	**Q4**	**Q1**	**Q2**	**Q3**	**Q4**
Procure crystals from Crytur	X	X			X	X		
Produce crystals at SIC	X	X						
Crystal quality tests			X	X	X	X		
Radiation Damage studies			X	X	X	X		
Construct prototype						X	X	
Test prototype								X

Table 2. Timeline of activities

5. Responsibilities

- CUA - Lead Institution. Coordination of R&D program. Procure $PbWO_4$ crystals from SIC and perform initial crystal quality measurements
- JLAB – provides facilities for radiation studies and quality measurements as needed
- BNL - Carry out radiation damage measurements (gamma ray and hadron). Study crystal readout using SiPMs
- Caltech – Perform crystal quality measurements and carry out gamma ray radiation damage studies
- IPN Orsay – procure PWO crystals from Crytur and perform initial crystal quality measurements in collaboration with University of Giessen
- Yerevan Physics Institute – Provides expertise with crystal quality measurements and comparison with other calorimeter crystal types, e.g., PbF_2 and existing $PbWO_4$

6. Funding Request and Budget

Item	Year 1 ($K)	Year 2 ($K)
Procure crystals from Crytur	30	60
Purchase crystals from SIC	15	
Gamma ray radiation studies	10	10
Hadron radiation studies	10	10
Technical Support	10	15
Parts for prototype		10
Travel	8	15
Total	**83**	**120**

Table 3. Funding by task

Institution	Year 1 ($K)	Year 2 ($K)
CUA	18	30
JLAB		
BNL	15	20
Caltech	15	20
IPN Orsay	35	50
Yerevan		
Total	**83**	**120**

Table 4. Funding by Institution

7. References

1. A. Accardi et al., "Electron-Ion Collider: The Next QCD Frontier – understanding the glue that binds us all", arXiv.1212.1701, BNL-98815-2012, JLAB-PHY-12-1652 (2012)
2. D. Boer et al., "Gluons and the sea quarks at high energies", arXiv.1108.1713, BNL-96164-2011, JLAB-PHY-11-1373 (2011)
3. EIC Wiki Page https://wiki.bnl.gov/eic/index.php/Main_Page
4. EIC Calorimeter Consortium Proposal (April 2012), Proposal 5, https://wiki.bnl.gov/conferences/index.php/Proposals-April2012
5. M. Kubantsev et al., Performance of the Primex Electromagnetic Calorimeter, arXiv:physics/0609201, 22 Sep. 2006; A. Gasparyan, Performance of PWO crystal Detector for a High Resolution Hybrid Electromagnetic Calorimeter at Jefferson Lab., Proceed. X Int. Conf. Calorimetry in Particle Physics, Perugia, Italy, 29 March-2 April 2004, pp. 109-115.
6. S. Abeyratne et al., "Science Requirements and Conceptual Design for a Polarized Medium Energy Electron-Ion Collider at Jefferson Lab", arXiv.1209.0775 (2012).
7. ePHENIX LoI, http://arxiv.org/abs/1402.1209
8. eSTAR LoI, https://drupal.star.bnl.gov/STAR/future/estar
9. EIC Dedicated Detector, https://wiki.bnl.gov/eic/index.php/ERHIC_Dedicated_Detector_Design
10. R.Y.~Zhu et al., Nucl. Inst.Meth A **413**, 297 (1998).

11. R.Y.~Zhu, IEEE Transactions on Nuclear Science, Vol 51, No. **4**, 2004; http://www.hep.caltech.edu/~zhu/papers/03_tns_pwo.pdf
12. Crytur, Czech Republic (http://www.crytur.cz/)
13. EIC Wiki Page https://wiki.bnl.gov/eic/index.php/Detector_Design_Requirements
14. Caltech Crystal Lab and Radiation Facility
15. BNL Gamma Ray Irradiation Facility, P.W.Levy, J. Chem. Phys. Solids, Vol. 52, No. 1 (1991) 319.
16. R.Y.~Zhu, IEEE Transactions on Nuclear Science, Vol 60, No. **3**, 2013; http://www.hep.caltech.edu/~zhu/papers/13_TNS_PWO-II.pdf
17. A. Barysevich et al., Nucl. Instr. and Meth. A **701** (2013) 231-234
18. V. Dormenev et al., Comparison of Radiation Damage Effects in PWO Crystals under 150 MeV and 24 GeV High Fluence Proton Irradiation, IEEE Trans. on Nucl. Sci. Vol 61, No. **1**, 2014, 501-506
19. NSRL http://www.bnl.gov/medical/nasa/nsrl_description.asp
20. "Radiation Hardness Test of SiPMs for the JLAB Hall D Barrel Calorimeter",Yi Quang et.al., Nucl. Inst. Meth. A698 (2013) 234-241; C. Zorn, "Proposal to test improved radiation tolerant silicon photomultipliers", (April 2011), Proposal 5 https://wiki.bnl.gov/conferences/images/c/c5/RD-5_EIC_JLAB_SiPM_Raddam_Proposal-all.pdf
21. "Influence of X-ray Irradiation on the Properties of the Hamamatsu Silicon Photomultiplier S10362-11-050C", C.Xu et.al, http://arxiv.org/abs/1404.3206
22. "Radiation Damage Studies on SiPMs for Calorimetry at the Super LHC", A.H.Herring et.al., 2008 IEEE NSS/MIC Conference Record Proceedings.
23. Indiana University Cyclotron Facility Low Energy Neutron Source (LENS), http://www.indiana.edu/~lens/
24. V. Popov and H. Mkrtchyan, New potomultiplier active base for Hall C Jefferson Lab Lead Tungstate Calorimeter, NSSS2012-1098.